International Journal of Physical Sciences Vol. 3 (1), pp. 038-041, January, 2008
Available online at http://www.academicjournals.org/IJPS
ISSN 1992 - 1950 © 2008 Academic Journals

Full Length Research Paper

Calculation of the Mie scattering field inside and outside a coated spherical particle

Honoh Suzuki* and I-Yin Sandy Lee

Department of Chemistry, University of Toyama, 3190 Gofuku Toyama 930-8555 Japan.

Accepted 25 January, 2007

A procedure to compute intensity distributions generated by the Mie scattering from a single coated sphere is described, and applied to a nanoshell and a microshell. The obtained information on the near-field intensity and the absorbed energy density is shown to be useful in predicting optical properties of the core-shell structure for applications.

Key words: Nanoparticles, Mie theory, near-field effects, absorbed energy density.

INTRODUCTION

Interactions of small particles with light have been an important subject in chemistry, astrophysics, biology, and electrical engineering (Bohren and Huffman, 1998). A recent advent of various forms of nanostructures allows us to control laser-particle interactions and manipulate the optical field in microscopic domains to alter nonlinear optical responses. One of the promising examples of engineered nanostructures is a so-called nanoshell, which is composed of a dielectric nanoparticle core surrounded by metallic coating (Jackson and Halas, 2001). If the coating is thin enough, the core-shell structure substantially alters the absorption and scattering properties of the particle. For example, a silver-silica nanoshell exhibits a surface-plasmon absorption band that is strongly red-shifted into the near-infrared (NIR) region, which makes this sort of nanomaterial attractive for use in optical communications and biomedical applications (Suzuki et al., 2006).

The electromagnetic interaction of a single spherical particle with light can be described by the Mie theory (Mie, 1908), which is a rigorous solution to the classical Maxwell equations. A coated sphere is also one of the simplest problems that can be solved by a straightforward extension of the theory. The available standard theory and computer programs usually focus on the far-field properties of the scattered optical field, such as the scattering efficiency, which is the most needed for optical and astrophysical purposes; however, a less attention has been paid to the near-field intensity distribution inside and in the vicinity of the scatterer (Barber and Hill, 1990).

*Corresponding author. E-mail:honoh@sci.u-toyama.ac.jp.

Such micro- and mesoscopic information is especially desirable in studies of enhancement of photo-induced physicochemical processes at localized sites near the particle surface, e.g., surface-enhanced Raman scattering, laser-induced breakdown, and cavity-field effects.

In this study, we present a suitable set of equations of the Mie theory extended to a coated sphere, with applications to nanoshells and microshells in mind. A computer program is described, which is designed for calculation of the near-field intensity distributions and also the absorbed energy density at an arbitrary position inside and outside of the scatterer.

Theory

Our formulation for a coated sphere is based on the Aden-Kerker extension of the Mie theory (Aden and Kerker, 1951; Bohren and Huffman, 1998). Suppose that a plane polarized electromagnetic wave is incident on a coated sphere with an inner radius "*a*" and an outer radius "*b*". We take the origin at the sphere center, the *z*-axis in the incident direction, and the *x*-axis in the polarization direction. The basic assumption to be made is that the core, the shell, and the medium are homogeneous, isotropic and linear; thus, the macroscopic Maxwell equations and the constitutive relations are valid. They are also assumed to be electromagnetically source-free. A rigorous solution to the Maxwell equations can be obtained via expansion in vector spherical harmonics. The electromagnetic fields inside the inner core ($\boldsymbol{E}_1$, $\boldsymbol{H}_1$) ($0 \le r \le a$), in the shell region ($\boldsymbol{E}_2$, $\boldsymbol{H}_2$) ($a \le r \le b$), and scattered away from the sphere ($\boldsymbol{E}_s$, $\boldsymbol{H}_s$) ($b \le r$) are written as:

$$\boldsymbol{E}_1 = \sum_{n=1}^{\infty} E_n (c_n \boldsymbol{M}_{o1n}^{(1)} - i d_n \boldsymbol{N}_{e1n}^{(1)}) \quad , \quad (1)$$

$$\boldsymbol{H}_1 = -\frac{k_1}{\omega \mu_1} \sum_{n=1}^{\infty} E_n (d_n \boldsymbol{M}_{e1n}^{(1)} + i c_n \boldsymbol{N}_{o1n}^{(1)}) \quad , \quad (2)$$

$$\boldsymbol{E}_2 = \sum_{n=1}^{\infty} E_n (f_n \boldsymbol{M}_{o1n}^{(1)} - i g_n \boldsymbol{N}_{e1n}^{(1)} + v_n \boldsymbol{M}_{o1n}^{(2)} - i w_n \boldsymbol{N}_{e1n}^{(2)}) \quad , (3)$$

$$\boldsymbol{H}_2 = -\frac{k_2}{\omega \mu_2} \sum_{n=1}^{\infty} E_n (g_n \boldsymbol{M}_{e1n}^{(1)} + i f_n \boldsymbol{N}_{o1n}^{(1)} + w_n \boldsymbol{M}_{e1n}^{(2)} + i v_n \boldsymbol{N}_{o1n}^{(2)}) \quad , \quad (4)$$

$$\boldsymbol{E}_s = \sum_{n=1}^{\infty} E_n (i a_n \boldsymbol{N}_{e1n}^{(3)} - b_n \boldsymbol{M}_{o1n}^{(3)}) \quad , \quad (5)$$

$$\boldsymbol{H}_s = \frac{k}{\omega \mu} \sum_{n=1}^{\infty} E_n (i b_n \boldsymbol{N}_{o1n}^{(3)} + a_n \boldsymbol{M}_{e1n}^{(3)}) \quad , \quad (6)$$

Where $E_n = i^n E_0 (2n+1)/[n(n+1)]$ with E_0 the incident field amplitude; ω is the angular frequency, k_1 the complex wave number in the core, k_2 in the shell, and k in the medium; μ_1, μ_2, and μ are the corresponding permeabilities. The standard (Bohren-Huffman) notation is used for the vector spherical harmonics $\boldsymbol{M}$ and $\boldsymbol{N}$, which are the functions of the spherical coordinates (r, θ, φ). We further assume that the surrounding medium is non-absorbing and that the particle is non-magnetic and carries no net surface charge. The eight scattering coefficients (a_n, b_n, c_n, d_n, f_n, g_n, v_n, w_n) are then obtained from the boundary conditions:

$$a_n = \frac{\psi_n(y)(\tilde{D}_n y + m_2 n) - m_2 y \psi_{n-1}(y)}{\xi_n(y)(\tilde{D}_n y + m_2 n) - m_2 y \xi_{n-1}(y)} \quad , \quad (7)$$

$$b_n = \frac{\psi_n(y)(\tilde{G}_n m_2 y + n) - y \psi_{n-1}(y)}{\xi_n(y)(\tilde{G}_n m_2 y + n) - y \xi_{n-1}(y)} \quad , \quad (8)$$

$$c_n = \frac{y[m_2 x D_n(x_2)\psi_n(x_2) - m_2 x B_n \chi_n(x_2) + n B_n \chi_n(x_2)][\psi_{n-1}(y)\xi_n(y) - \psi_n(y)\xi_{n-1}(y)]}{x D_n(x_1)\psi_n(x_1)[\psi_n(y_2) - B_n \chi_n(y_2)][m_2 y \tilde{G}_n \xi_n(y) - y \xi_{n-1}(y) + n \xi_n(y)]} \quad , (9)$$

$$d_n = \frac{m_2 y [\psi_n(x_2) - A_n \chi_n(x_2)][\psi_{n-1}(y)\xi_n(y) - \psi_n(y)\xi_{n-1}(y)]}{\psi_n(x_1)[\psi_n(y_2) - A_n \chi_n(y_2)][y \tilde{D}_n \xi_n(y) - m_2 y \xi_{n-1}(y) + m_2 n \xi_n(y)]} \quad , (10)$$

$$f_n = \frac{m_2 y [\psi_{n-1}(y)\xi_n(y) - \psi_n(y)\xi_{n-1}(y)]}{[\psi_n(y_2) - B_n \chi_n(y_2)][m_2 y \tilde{G}_n \xi_n(y) - y \xi_{n-1}(y) + n \xi_n(y)]} \quad , (11)$$

$$g_n = \frac{m_2 y [\psi_{n-1}(y)\xi_n(y) - \psi_n(y)\xi_{n-1}(y)]}{[\psi_n(y_2) - A_n \chi_n(y_2)][y \tilde{D}_n \xi_n(y) - m_2 y \xi_{n-1}(y) + m_2 n \xi_n(y)]} \quad , \quad (12)$$

$$v_n = \frac{m_2 y B_n [\psi_{n-1}(y)\xi_n(y) - \psi_n(y)\xi_{n-1}(y)]}{[\psi_n(y_2) - B_n \chi_n(y_2)][m_2 y \tilde{G}_n \xi_n(y) - y \xi_{n-1}(y) + n \xi_n(y)]} \quad , \quad (13)$$

$$w_n = \frac{m_2 y A_n [\psi_{n-1}(y)\xi_n(y) - \psi_n(y)\xi_{n-1}(y)]}{[\psi_n(y_2) - A_n \chi_n(y_2)][y \tilde{D}_n \xi_n(y) - m_2 y \xi_{n-1}(y) + m_2 n \xi_n(y)]} \quad , \quad (14)$$

where $x = 2\pi aN/\lambda$ and $y = 2\pi bN/\lambda$ are the size parameters of the core and the shell, N the refractive index of the medium, λ the wavelength, $x_1 = m_1 x$, $x_2 = m_2 x$, $y_2 = m_2 y$; m_1 and m_2 are the complex refractive index of the core and the coating, respectively, relative to the medium. ψ_n, ξ_n, and χ_n are the Riccati-Bessel functions, and $D_n = \psi_n'/\psi_n$ is the logarithmic derivative. A_n, B_n, $\tilde{D}_n$, and $\tilde{G}_n$ are functions defined for computational convenience, which can be found in the literature (Bohren and Huffman, 1998).

With the knowledge of the size and optical constants of the component materials, the fields at an arbitrary position inside and outside of the coated sphere can be calculated with the above set of equations. The total field outside the sphere is the sum of the scattered field ($\boldsymbol{E}_s$, $\boldsymbol{H}_s$) and the incident field ($\boldsymbol{E}_i$, $\boldsymbol{H}_i$):

$$\boldsymbol{E}_i = E_0 \exp(ikr\cos\theta)\hat{\boldsymbol{e}}_x \quad , \quad (15)$$

$$\boldsymbol{H}_i = \frac{k}{\omega \mu} E_0 \exp(ikr\cos\theta)\hat{\boldsymbol{e}}_y \quad . \quad (16)$$

Since our primary interest in the near-field of the scatterer is in nonlinear effects and local energy deposition due to the localized strong field, we calculate the spatial distributions of the intensity (field amplitude squared) $|\boldsymbol{E}|^2$ and also of the absorbed energy density U as a function of the position. The latter is equal to the negative divergence of the time-averaged Poynting vector $\boldsymbol{S}$:

$$U = -div\,\boldsymbol{S} = -\frac{1}{2} Re[\nabla \cdot (\boldsymbol{E} \times \boldsymbol{H}^*)] = \frac{1}{2}\omega[Im(\mu)\boldsymbol{H}\cdot\boldsymbol{H}^* + Im(\varepsilon)\boldsymbol{E}\cdot\boldsymbol{E}^*] \quad , \quad (17)$$

where ε is the permittivity, and the second line is derived by using the vector derivative identity $\nabla\cdot(A\times B) = B\cdot(\nabla\times A) - A\cdot(\nabla\times B)$ and the Maxwell

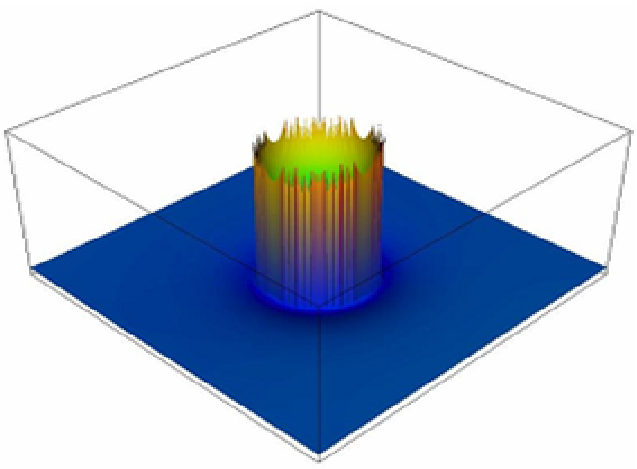

Figure 1. Intensity distribution of a nanoshell irradiated at 1064 nm in water. The nanoshell has a silica core with a diameter of 100 nm and a 10 nm thick silver shell.

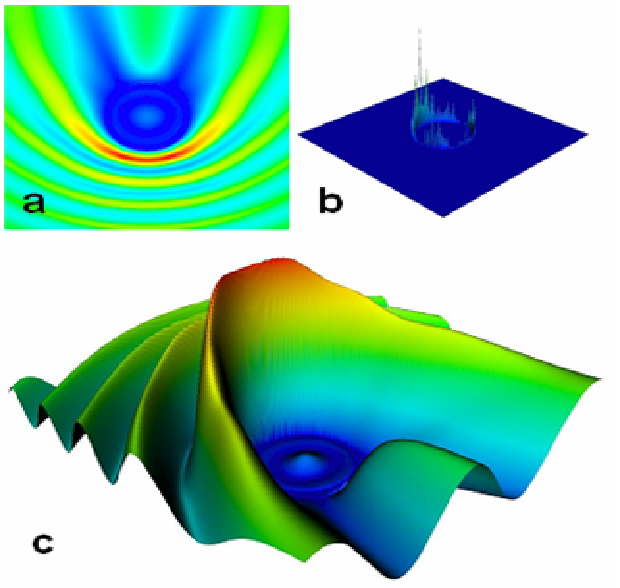

Figure 2. Intensity distribution of a silica-silver microshell irradiated at 1064 nm in water, with a core diameter of 1 μm and a shell thickness of 100 nm. (a) Colored surface map of intensity. The incident direction is from bottom to top. (b) Distribution of the absorbed energy density. (c) Three-dimensional map of intensity inside and outside the microshell.

equations. As we assume that the particle is non-magnetic, it follows from $Im(\varepsilon) = 2\varepsilon_0 nk$ that :

$$U = \varepsilon_0 \omega nk |E|^2 , \quad (18)$$

where $N = n + ik$ is the complex refractive index at the position. In the case of a homogeneous plane wave, this expression coincides with a familiar product form of the intensity (irradiance) multiplied by the absorption coefficient, $U = \alpha I$, since $\alpha = 4\pi k/\lambda$ and $I = \frac{1}{2} Re(\sqrt{\varepsilon/\mu}) |E|^2$.

Computational details

Our program (BHFIELD) (Suzuki, 2007) is an extended version of the standard Fortran codes (BHCOAT) (Bohren and Huffman, 1998), in which several improvements and modifications have been made to allow the field calculations.

First, wavelength-dependent optical constants of materials are loaded from the literature data set, from which accurate values are determined for each wavelength of interest by interpolation. A correction to the bulk optical constants for small metal particles is also taken into account. Although the bulk refractive index is valid in most small particles, i.e., the quantum size effects are unimportant well below the size of 100 nm, it is known that, in metal particles smaller than the mean free path of conduction electrons, the free-electron term in the dielectric function is modified because of the limited free path by collisions with the particle boundary (Bohren and Huffman, 1998). This effect is especially important in silver and aluminum, and in the case of nanoshells in which the silver coating tends to be quite thin. We use a procedure proposed by Kreibig for such corrections (Kreibig, 1974).

Second, we use a different recurrence algorithm to calculate the spherical Bessel functions j_n and y_n, and the logarithmic derivative D_n. It is known that j_n and D_n are numerically unstable with respect to upward recurrence, whereas y_n is upward stable. The original algorithm uses upward recurrence for all of them, which is tolerable for the calculation of scattering efficiencies, but not suitable for the external field calculation where a large distance is encountered and thus higher series terms in the summation (typically $n > 50$) are required. Accordingly, we use downward recurrence for j_n and D_n and upward one for y_n, which allows us to satisfactorily compute the external field beyond the nearest-field region, and also to eliminate the need for subtle cut-off criteria (to avoid the recurrence instability) incorporated in the original codes. We also note that the use of high precision variables (both real and complex) is critical to avoid over- and underflow problems in the computation.

RESULTS AND DISCUSSION

We have calculated the intensity distribution for two typical examples that have a coated structure: a nanoshell (Figure 1) and a microshell (Figure 2). The optical constants are taken from the literature (Segelstein, 1981; Palik, 1997). Although both are composed of a silica core and a silver shell, they exhibit significantly different characteristics in the near-field profiles, according to the core size and the shell thickness. The nanoshell (core diame-

ter 100 nm, shell thickness 10 nm) is small compared with the wavelength of 1064 nm, thus closer to the Rayleigh limit. The intensity in the silver shell region is highly enhanced, being almost 20 times stronger than the incident intensity (Figure 1). The intensity is also fairly uniform inside the shell, i.e., interference and shading effects are minor. The absorbed energy density in the shell is also large and uniform; it is more than doubled after the Kreibig free-path correction has been made. It suggests that nanoshells of this size can be strong near-infrared absorbers, which are optically heated up in the shell region in an isotropic manner (Suzuki et al., 2006).

On the other hand, the microshell (core diameter 1 μm, shell thickness 100 nm) strongly scatters the incident light, with an excessive fringe pattern in the near-field (Figure 2). It may be a combined effect of the larger size and the thicker silver layer, which expels the incident light from both the core and shell regions of the particle. As a result, both the intensity and the absorbed energy density in the shell region are six orders of magnitude lower than those in the nanoshell. The profile inside the shell is also anisotropic, showing interference and shadow effects (Figure 2b). Therefore, such microshells may be more useful as near-field scatterers (and possibly image-enhancers) than absorbers.

Conclusion

We have described a procedure for calculation of the spatial profile of intensity scattered from a coated sphere by the Mie-Aden-Kerker theory. It gives a clear picture of the size effect, that is, the significant difference between a nanoshell and a microshell in the near-field profiles. It is useful in interpreting, predicting, and tailoring optical properties of nanoshells and microshells for future applications in nonlinear optics, photocatalysis, and biomedical applications.

ACKNOWLEDGMENTS

This work is supported by the Japanese Ministry of Education, Science and Culture (Grant Nos. 15750115 and 17510086).

REFERENCES

Aden AL, Kerker M (1951). Scattering of Electromagnetic Waves from Two Concentric Spheres. J. Appl. Phys. 22: 1242-1246.

Barber PW, Hill SC (1990). Light Scattering by Particles: Computational Methods. World Scientific.

Bohren CF, Huffman DR (1998). Absorption and Scattering of Light by Small Particles. Wiley-Interscience.

Jackson J, Halas N (2001). Silver Nanoshells: Variations in Morphologies and Optical Properties. J. Phys. Chem. B105: 2743-2746.

Kreibig U (1974). Electronic properties of small silver particles: the optical constants and their temperature dependence. J. Phys. F 4: 999-1014.

Mie G (1908). Beiträge zur Optik trüber Medien, speziell kolloidaler Metallösungen. Ann. Phys. 25: 377-445.

Palik ED (1997). Handbook of Optical Constants of Solids. Academic Press.

Segelstein DJ (1981). The complex refractive index of water. M. S. Thesis, University of Missouri, Kansas City.

Suzuki H (2007). BHFIELD: A Fortran program for the Mie field calculation. University of Toyama.

Suzuki H, Koike T, Suzuki I, Kawabata T, Lee IYS (2006). Localization of laser-induced breakdown in aggregates of silver nanoshells. Sci. Technol. Adv. Mater. 7: 290-295.